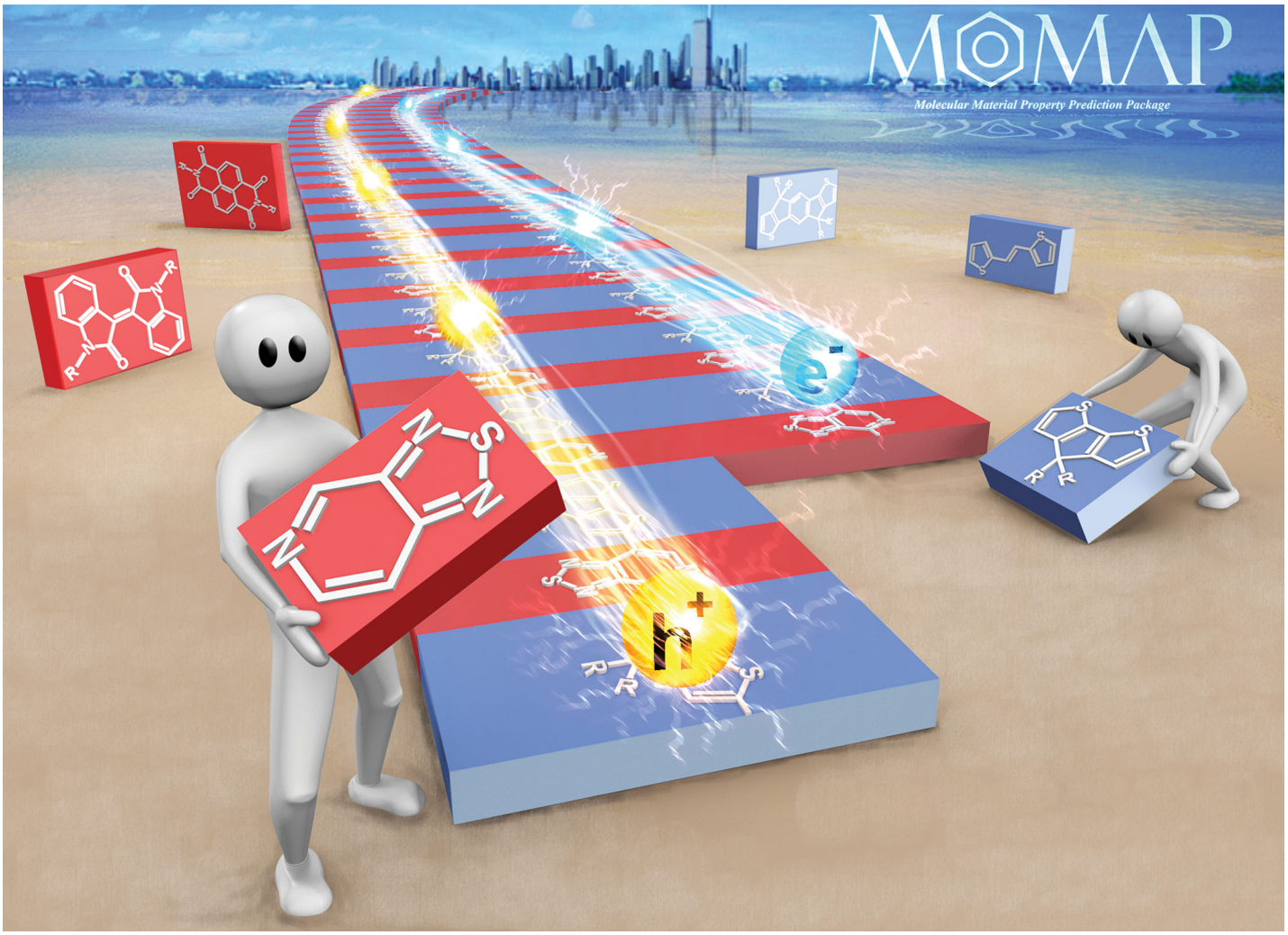

Showcasing research from the Shuai group at Tsinghua University and Institute of Chemistry, Chinese Academy of Sciences.

Super-exchange-induced high performance charge transport in donor–acceptor copolymers

The recently discovered ultra-high carrier mobility in donor–acceptor copolymers is rationalized from the super-exchange mechanism. A molecular design strategy for high mobility copolymers is put forward.

As featured in:

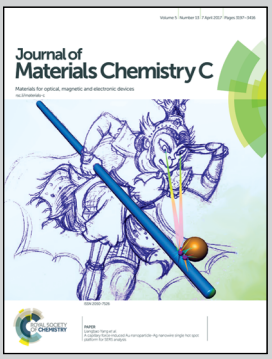

See Hua Geng, Zhigang Shuai *et al.*, *J. Mater. Chem. C*, 2017, **5**, 3247.

ROYAL SOCIETY OF CHEMISTRY

rsc.li/materials-c

Registered charity number: 207890

Journal of Materials Chemistry C

PAPER

View Article Online
View Journal | View Issue

Cite this: J. Mater. Chem. C, 2017, 5, 3247

Super-exchange-induced high performance charge transport in donor–acceptor copolymers†

Changli Cheng,[a] Hua Geng,*[b] Yuanping Yi[b] and Zhigang Shuai*[a]

Received 22nd December 2016,
Accepted 14th February 2017

DOI: 10.1039/c6tc05534f

rsc.li/materials-c

Based on the super-exchange (SE) model and first-principles computations, we demonstrate that donor–acceptor copolymers can intrinsically possess an ultra-small effective mass due to the SE effect, rationalizing the recent experimental demonstration of ultra-high charge mobility. With the increase of the SE coupling, the effective mass decreases correspondingly. For the first time, we report that the SE coupling for holes is determined by the dihedral angle between the donor and the acceptor moiety, HOMO charge density at the linkage site and the HOMO–LUMO gap of the bridge fragment. Thereby, we put forward a molecular design strategy for large SE coupling so as to obtain an ultra-small effective mass. Finally, by combining a variety of donor and acceptor groups, we predict that several D–A copolymers can potentially possess an ultra-low effective mass due to the long range SE effect, and are expected to be high charge mobility polymers.

Introduction

Organic conjugated polymers have been widely used in organic photovoltaics (OPVs) and organic field effect transistors (OFETs) for the emerging printing electronics applications.[1] In recent years, a variety of donor–acceptor copolymers have been demonstrated with high charge mobility.[2–5] For instance, by copolymerizing benzothiadiazole (BT) with indacenodithiophene (IDT), the McCulloch group showed that the hole FET mobility of IDT-BT reaches $\sim$3.6 $cm^2\ V^{-1}\ s^{-1}$.[5] Heeger *et al.* found that the hole FET mobility of cyclopentadithiophene-pyridinethiadiazole (CDT-PT) even exceeds 50 $cm^2\ V^{-1}\ s^{-1}$,[6] the state-of-the-art mobility for polymeric semiconductors. The most recent experiments indicate that the charge transport mainly presents quasi-one-dimensional character along the polymer backbone coupled with very few occasional intermolecular hopping.[5,7] It is also demonstrated that the transport polarity, being p-type or n-type, can be tuned by the acceptor group.[8] By combining different donor and acceptor units for copolymerization, the charge mobility has been found to range from 10^{-2} to dozens of $cm^2\ V^{-1}\ s^{-1}$.[3,8–14] It is intriguing to understand the effects of various donor and acceptor combinations on the electronic structures in order to gain insights into the molecular design for high charge mobility polymers.

The underlying charge transport mechanism in D–A copolymers remains unclear. Fornari and Troisi have proposed a mechanism based on the reduced barrier between the mobility edge and the carrier energy level, namely, (i) the D–A polymer bandwidths are in general narrow; and (ii) polymers are always disordered in the electronic structure and there always exists a mobility edge. The narrow bandwidth implies a reduced energy barrier from the conducting carrier level to the mobility edge, leading to lowered activation energy for the hopping process.[15] However, photoemission experiment demonstrated that the bandwidth of D–A polymers is not narrow.[6] Also, more and more highly oriented polymers have been reported with a band-like transport behaviour, and a strong intra-chain electronic delocalization picture has been confirmed by a number of experimental studies.[9,16–19] The bandwidth originates from a synergistic effect of static disorder (or site energy distribution) and electronic coupling;[20] the former is detrimental but the latter is helpful for charge transport. Thus, it is difficult to judge charge transport properties from bandwidth only.

Since polymer chains possess large conformational freedom along the backbone, most polymers present amorphous conformations and low charge carrier mobility (10^{-5}–10^{-2} $cm^2\ V^{-1}\ s^{-1}$).[21] However, more recently, with the progress in material processing techniques, polymer nanowires and highly crystalline thin films have been prepared and remarkably high mobility has been demonstrated.[6,12,22] Therefore, we can regard the backbone of highly ordered polymers as a periodic structure. The carrier mobility can be expressed as $\mu = e\tau/m^*$, where τ is the scattering relaxation time which is inversely proportional to the charge scattering probability, e is the charge, and m^* is the effective mass. A small effective mass always implies large carrier mobility,

[a] MOE Key Laboratory of Organic OptoElectronics and Molecular Engineering, Department of Chemistry, Tsinghua University, Beijing 100084, China. E-mail: zgshuai@tsinghua.edu.cn
[b] Beijing National Laboratory for Molecular Sciences, CAS Key Laboratory of Organic Solids, Institute of Chemistry, Chinese Academy of Sciences, Beijing 100190, China. E-mail: hgeng@iccas.ac.cn

† Electronic supplementary information (ESI) available. See DOI: 10.1039/c6tc05534f

regardless of the transport mechanism. In this work, based on extensive first-principles electronic structure calculations, we propose a super-exchange mechanism to explain the high mobility phenomena in a series of donor–acceptor alternating copolymers. A design strategy for high mobility polymers can be proposed from such an understanding.

In D–A polymers, two donor (acceptor) groups are separated by one acceptor (donor) and are not directly coupled electronically. The effective coupling between adjacent donors (acceptors) is mediated by the in-between acceptor (donor), *i.e.*, *via* super-exchange (SE) coupling. We have noted that the bridge-mediated electron transfer has been found to play an essential role in long distance charge migration in DNA.[23] Here, we focus on the intra-chain SE coupling along the polymer backbone, and establish a structure–property correlation for ultra-small effective mass from a long range SE perspective. By maximizing SE coupling, we also predict that several D–A copolymers can potentially possess a small hole effective mass, smaller than that of CDT-PT. This work provides molecular insights into the origin of electronic couplings in alternating D–A copolymers, paving the way toward rational design of high-performance charge transport polymers.

Methodology

1. Electronic structure and effective mass

The geometry structures of the isolated polymer chain with 1D periodicity were optimized using the B3LYP functional and the 6-31G(d) basis set with the CRYSTAL14 code.[24] The uniform $21 \times 1 \times 1$ Monkhorst–Pack k-point mesh was employed for all D–A copolymers. To generate the band structures, 41 k-points were calculated between the gamma point (centre of the Brillouin Zone, BZ) and the edge of the first BZ. The effective mass for one-dimensional crystals is calculated from the band structure as follows:

$$m^* = \hbar^2 \Big/ \frac{\mathrm{d}^2 E}{\mathrm{d}k^2} \tag{1}$$

where E is the band energy and k is the electron wave vector along the backbone direction. To understand the origin of the ultra-small effective mass in D–A copolymers, we recall the one-dimensional tight-binding model. Donor and acceptor fragments are regarded as sites connected by covalent bonds. The bandwidth and effective mass of polymers can be written as

$$W = \begin{cases} 4V_{\mathrm{DA}} & \Delta\varepsilon = 0 \\ \sqrt{(\Delta\varepsilon/2)^2 + 4V_{\mathrm{DA}}{}^2} - \Delta\varepsilon/2 & \end{cases} = \begin{cases} 2V_{\mathrm{DA}} & 0 < \Delta\varepsilon \ll V_{\mathrm{DA}} \\ 4V^{\mathrm{eff}} & \Delta\varepsilon \gg V_{\mathrm{DA}} \end{cases} \tag{2}$$

$$m^* = \frac{\hbar^2}{a^2 V_{\mathrm{DA}}{}^2}\left[(\Delta\varepsilon/2)^2 + 4V_{\mathrm{DA}}{}^2\right]^{1/2} = \begin{cases} \dfrac{\hbar^2}{2(a/2)^2 V_{\mathrm{DA}}} & \Delta\varepsilon \ll V_{\mathrm{DA}} \\ \dfrac{\hbar^2}{2a^2 V^{\mathrm{eff}}} & \Delta\varepsilon \gg V_{\mathrm{DA}} \end{cases} \tag{3}$$

Here, $\Delta\varepsilon$ is the site energy difference between donor and acceptor units, a is the length of the unit cell, V_{DA} is the nearest neighbour direct coupling between donor and acceptor units, and $V^{\mathrm{eff}} = V_{\mathrm{DA}}{}^2/\Delta\varepsilon$ is the bond-mediated super-exchange coupling, where one site is represented by one orbital. In contrast to homopolymers ($\varepsilon \ll V_{\mathrm{DA}}$), where the effective mass is determined by the direct coupling (V_{DA}) between neighbouring fragments, the effective mass of D–A copolymers ($\varepsilon \gg V_{\mathrm{DA}}$) is defined by the super-exchange (SE) coupling V^{eff}.

2. Super-exchange coupling model in D–A copolymers

It is comprehensible that the effective mass of homopolymers is determined by direct electronic coupling. Here, it should be noted that the effective mass of D–A copolymers is determined by the length of the unit cell and the bond-mediated SE coupling; this bond-mediated SE coupling is similar to the situation in van der Waals stacked donor–acceptor cocrystals,[25,26] and thus, it is especially important to evaluate intra-chain SE coupling from quantum chemistry calculations. The partition-based approach, implemented by us, has been adopted to compute SE coupling to unravel the transport polarity in organic D–A cocrystals.[26] This method can not only account for the site energy correction from the polarization effect of the environment, but also can take the contributions from each individual molecular orbital of the bridge into consideration. Due to the electrostatic interaction and charge transfer between donors and acceptors, the effect of electrostatic polarization and site energy correction on SE coupling should be considered. Thus, the simple energy splitting method for evaluating SE cannot be applied. We calculate the super-exchange coupling for holes based on a DAD oligomer triad, and for electrons, based on an ADA triad, as shown in Scheme 1.

The electronic properties of the triad oligomers are described by a secular equation in terms of donor and acceptor fragment orbitals with hydrogen passivation. The fragment molecular orbital coefficients were normalized without hydrogen. The Hamiltonian

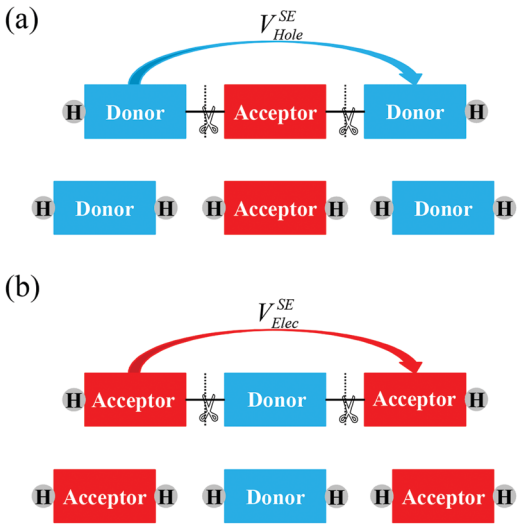

Scheme 1 Theoretical models of D–A–D (a) and A–D–A (b) oligomers for hole and electron super-exchange coupling calculations.

of the triad system can be projected to above normalized orbitals.

$$H = \begin{pmatrix} \varepsilon_1 & V_{12} & V_{1B} \\ V_{21} & \varepsilon_2 & V_{2B} \\ V_{B1} & V_{B2} & \varepsilon_B \end{pmatrix} \quad (4)$$

$$S = \begin{pmatrix} 1 & S_{12} & S_{1B} \\ S_{21} & 1 & S_{2B} \\ S_{B1} & S_{B2} & 1 \end{pmatrix} \quad (5)$$

The matrix elements in eqn (4) and (5) can be calculated as follows:

$$\varepsilon_i = \langle \psi_i | H | \psi_i \rangle \quad (6)$$

$$V_{ij} = V_{ji} = \langle \psi_i | H | \psi_j \rangle \quad (7)$$

$$S_{ij} = S_{ji} = \langle \psi_i | \psi_j \rangle \quad (8)$$

Here, ψ_{ij} denotes the oligomer triad orbitals localized on donor or acceptor moieties, which are constructed using the respective isolated molecular orbital of hydrogen saturated donor and acceptor moieties. For hole (electron) transport, ψ_1 and ψ_2 are the HOMO (LUMO) of D1 (A1) and D2 (A2), respectively, and ψ_B represents the molecular orbitals of the bridge A (D) fragment. The Hamiltonian based on an orthogonalized basis can be then obtained by means of Löwdin's symmetric transformation:[26]

$$\tilde{H} = S^{-1/2} H S^{-1/2} = \begin{pmatrix} \tilde{\varepsilon}_1 & \tilde{V}_{12} & \tilde{V}_{1B} \\ \tilde{V}_{21} & \tilde{\varepsilon}_2 & \tilde{V}_{2B} \\ \tilde{V}_{B1} & \tilde{V}_{B2} & \tilde{\varepsilon}_B \end{pmatrix} \quad (9)$$

Next, by utilizing the Larsson partition technique in connection with the perturbation scheme, we obtain the effective electronic coupling. The effective SE coupling is composed of two parts: implicit and explicit couplings:

$$V^{\mathrm{eff}} = V^{\mathrm{im}} + \sum_{b \in B} \frac{\tilde{V}_{1b} \tilde{V}_{b2}}{E - \tilde{\varepsilon}_b} \quad (10)$$

Here, the implicit term (V^{im}) is the Hamiltonian matrix element obtained through projection Hamiltonian of the triad system on an orthogonalized fragment basis. It is null if no bridge is presented. The implicit term is substantially weaker than the explicit counterpart for D–A polymers. $\hat{V}_{1b}$ and $\hat{V}_{b2}$ denote the coupling of the bridge orbital (b) with the frontier orbitals of the two adjacent fragments (1 and 2); E and $\tilde{\varepsilon}_b$ correspond to the energies of the adiabatic and bridge levels in the triad oligomer, respectively.

The calculations of oligomers were performed by using the B3LYP functional and the 6-31G(d) basis set with GAUSSIAN 09 code.[27] It has been found that the present partition method is robust against the system size. For instance, going from a DAD (or ADA) triad to DADADA, even though the frontier molecular levels undergo a remarkable change, the calculated SE coupling constants are very similar, as can be seen from Fig. S1 (ESI†), well justifying the application of our method.

Results and discussion

D–A copolymers consist of a combination of π-electron-rich donors and π-electron-deficient acceptors arrayed along the polymer chain. Several π-electron-deficient conjugated moieties, such as benzothiadiazole (BT), isoindigo (IID), naphthalenediimide (NDI) and pyridal[2,1,3]-thiadiazole (PT), are extensively employed as acceptors.[6,13,28] As far as donors are concerned, the π-electron-rich moieties, for instance, 2T, (*E*)-2-(2-(thiophen-2-yl)vinyl)-thiophene (TVT), indacenodithiophene (IDT), and cyclopentadithiophene (CDT), when coupled with different acceptors, have been found to display high charge mobility in FET devices.[2,6,29] The combination of PT with CDT presents the state-of-the-art mobility for polymeric semiconductors.[6] In addition, we have also considered donor moieties, including 4T, TTTT (four-fused thiophenes), pyrene (Py), and fluorene (Flu), and acceptor moieties, including [1,2,5]thiadiazolo[3,4-*g*]quinoxaline (TDQ), tetrafluorophenylene (4FPh), and $(CF_2)_4$. Therefore, in total, we built fifty-six D–A alternating copolymer structures from seven acceptors and eight donor moieties, as shown in Scheme 2.

According to the literature, most of the BT and PT based D–A copolymers reveal coplanar conformation.[2,5,6,30] There exist *cis* and *trans* conformations depending on the torsion angle between donor and acceptor units. Similar energies and electronic structures have been found for the two conformations.[30] And thus, we adopt *trans* conformation as our theoretical model for these coplanar cases, as shown in Fig. S2 (ESI†). The effective mass of *cis* conformation for IDT-BT has also been listed in Table S1 (ESI†). Meanwhile, IID, NDI, Flu and Py based copolymers are nonplanar and there exist two energy minima from torsional potential calculations.[28,31–33] For nonplanar copolymers, the global minimum energy conformation has been chosen as our theoretical model. There may exist some static and dynamic

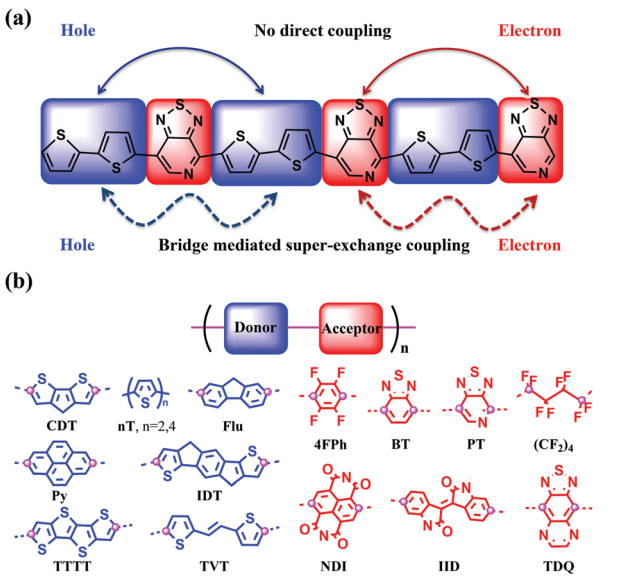

Scheme 2 (a) Super-exchange mechanism in a D–A alternating copolymer. (b) Chemical structure of donor and acceptor fragments. The linkage sites in both donor and acceptor are marked by circles.

disorders in D–A copolymers, such as relative orientation and torsional rotation between donor and acceptor units. These are beyond the scope of this work, and deserve further discussion in the future.

We noted that for NDI, IID, Flu and Py based copolymers, there exists a large torsional angle between the donor and acceptor moieties owing to the steric hindrance effect, while other D–A copolymers display a nearly coplanar structure along the backbone. It has been found that the bond length between D and A moieties is the shortest for TDQ-based copolymers, and increases for PT and BT based copolymers, and then for NDI and IID based copolymers (see Table S2 (ESI†)). From the electronic band structures, the valence (conduction) bands are mainly composed of the HOMO (LUMO) of the donor (acceptor) moiety coupled with the orbitals of the bridge moiety, as can be seen in Fig. 1(a). CDT-PT and TDQ based copolymers reveal a relatively large bandwidth (~1.3 eV), which is less than that of the typical homopolymer P3HT (~2.03 eV).[34] It has been observed that the bandwidths of both valence and conduction bands are linearly dependent on SE coupling (Fig. 1(b)), in agreement with eqn (2), indicating the suitability of our bridge-mediated SE interaction in these copolymers.

Based on the first-principles band structure calculations, the hole effective mass at the top of the valence band can be obtained from eqn (1). Hole (electron) SE couplings of DAD (ADA) oligomers have been performed based on the Larsson partition technique from eqn (10). To understand the effect of SE coupling on charge transport properties, effective mass and SE coupling are shown in Fig. 2.

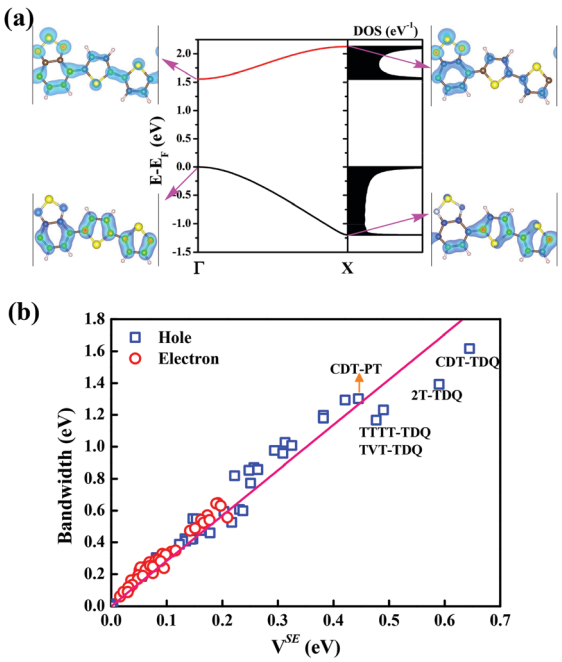

Fig. 1 (a) Band structure, density of states, and partial charge density at high symmetry points for 2T-BT. (b) The dependence of bandwidth on SE coupling for different D–A copolymers. The bandwidth and SE coupling are obtained from first-principles calculations using the CRYSTAL and GAUSSIAN code, respectively.

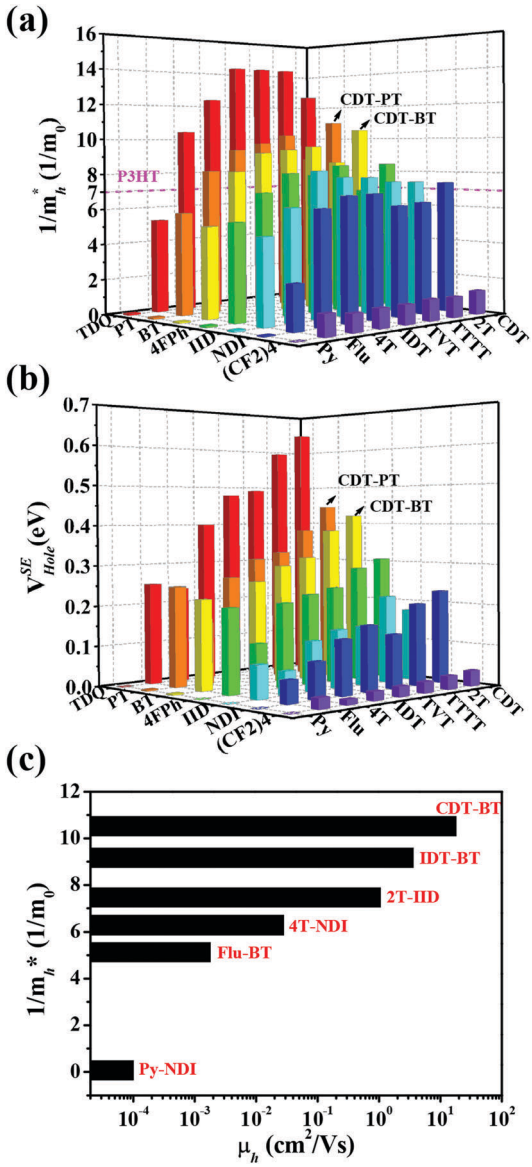

Fig. 2 (a) Inverse of the hole effective mass from periodic band structure calculations at the B3LYP/6-31G(d) level using the CRYSTAL code (m_0 is the mass of a bare electron). (b) Hole super-exchange coupling calculated from a DAD oligomer triad at the B3LYP/6-31G(d) level using the GAUSSIAN code. (c) Correlation between the first-principles calculated hole effective mass and experimentally measured hole mobility.

It has been noted that most of the D–A copolymers possess even smaller effective mass than that of homopolymers (about $0.14m_e$ for P3HT),[35] as shown in Fig. 2(a). Comparing Fig. 2(a) and (b), it is found that in general, large SE coupling and a long inter-unit distance lead to an small effective mass. As seen in Fig. S4 (ESI†), in the case of acceptor moieties with a similar length (except IID), the larger the SE coupling (in PT, BT and TDQ based copolymers), the smaller the effective mass. Likewise, for small SE coupling (in $(CF_2)_4$, NDI, IID, Flu and Py based copolymers), the resulting effective masses are relatively large, in full agreement with eqn (3). The state-of-the-art experimental FET mobility (~50 cm^2 V^{-1} s^{-1}) has been found for CDT-PT,

while CDT-BT displays comparable average mobility with CDT-PT under the same experimental conditions.[6] From Fig. 2(a), CDT-PT indeed possesses a small effective mass ($\sim 0.091 m_e$), which is close to the experimentally measured value based on angle resolved photoemission spectroscopy ($\sim 0.106 m_e$).[16] CDT-BT possesses a nearly equal effective mass ($\sim 0.095 m_e$) to CDT-PT, which rationalizes the comparable charge transport properties of CDT-PT and CDT-BT. Moreover, high intra-chain charge mobility (~ 3.6 cm^2 V^{-1} s^{-1}) was also reported for IDT-BT,[5] which possesses a small effective mass ($0.109 m_e$) (Fig. 2), justifying the experiment. In addition, Flu-BT, 2T-NDI, and 4T-NDI have been reported with charge mobility ranging from 10^{-3} to 10^{-2} cm^2 V^{-1} s^{-1}.[13,36,37] It is clear from Fig. 2 that their effective masses fall in the middle range. Py-NDI has been reported with mobility as low as $\sim 10^{-4}$ cm^2 V^{-1} s^{-1},[38] and the effective mass was indeed found to be the largest one ($14.7 m_e$) here. We can safely state here that there is indeed a strong correlation between the calculated effective mass and the measured carrier mobility for D–A copolymers. The correlation between experimentally measured mobility and effective mass is plotted in Fig. 2(c).

Most interestingly, we found that the TDQ moiety could surpass PT based copolymers with lower effective mass. When TDQ is coupled with CDT, 2T, TTTT, TVT and IDT, significant super-exchange couplings are demonstrated, especially for 2T, TVT and TTTT, revealing the smallest effective mass among all copolymers due to the large SE coupling. And thus, with the increase of SE coupling, the effective mass decreases correspondingly.

Now we look at the conditions leading to strong SE coupling at the molecular level. Since SE coupling mainly comes from the π-orbital of the bridge part, we can employ the tight binding Hückel approximation to express the second term of eqn (10) explicitly as follows:

$$V^{\mathrm{eff}}_{\mathrm{Hole/Elec}} \propto C^{\mathrm{D1(A1)}} C^{\mathrm{Dn(An)}} \cos(\phi_{\mathrm{DA}}) \cos(\phi_{\mathrm{AD}}) \sum_{\nu \in \mathrm{A(D)}} \frac{C_\nu^{\mathrm{A1(D1)}} C_\nu^{\mathrm{An(Dn)}}}{E - \varepsilon_\nu^{\mathrm{A(D)}}} \quad (11)$$

Here, C is the molecular orbital coefficient. D (A)$_1$ and D (A)$_n$ are the left and right linkage sites of the donor (acceptor), respectively. ϕ_{DA} denotes the torsional angle between the π-orbital of the donor and the acceptor unit. E and $\varepsilon_\nu^{\mathrm{A(D)}}$ correspond to the energy of the adiabatic orbital in the triad oligomer and the energy of the acceptor (donor) moiety, respectively. The summation runs over all molecular orbitals of the bridge. In the case of an axial-symmetry system, $C^{\mathrm{D1}}_{\mathrm{HOMO}} = C^{\mathrm{Dn}}_{\mathrm{HOMO}}$ and $\cos(\phi_{\mathrm{DA}}) = \cos(\phi_{\mathrm{AD}})$. The coefficient $C^{\mathrm{D1(A1)}} C^{\mathrm{Dn(An)}}$ is equal to $\rho^{\mathrm{D1(A1)}}_{\mathrm{HOMO(LUMO)}}$. SE coupling depends on the charge density at the linkage site and the torsional angle ϕ_{DA} between the molecular orbital of the donor and acceptor.

Due to the steric effect, for NDI, Flu, Py and IID based copolymers, large torsional angles are present and thereby relatively small SE coupling is found. From eqn (11), the contribution from the bridge contains a summation over molecular levels of the bridge and the numerator is a product of MO coefficients. Thus, the relative phases and the relative alignment of donor orbitals with respect to the bridge orbitals determine the sign of each term in the summation. Often, the HOMO (LUMO) of the donor (acceptor) lies within the HOMO–LUMO gap of the bridge. Thus, both HOMO and LUMO levels of the bridge play the most important role in charge transport. The respective contribution from each MO of the bridge is shown in Fig. 3.

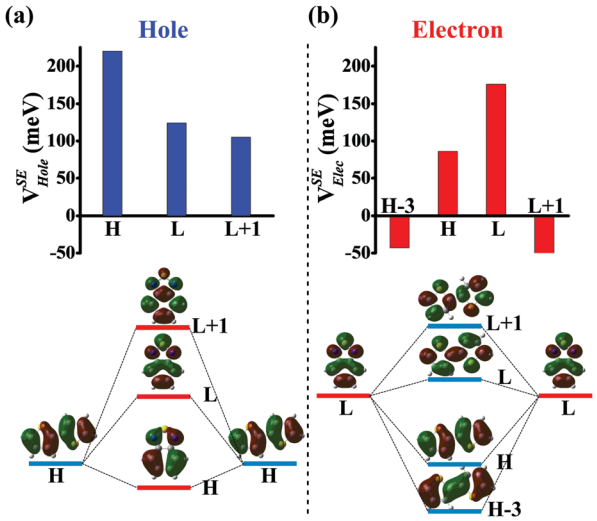

Fig. 3 Illustration of the contribution of the molecular orbital of the bridge to SE couplings for holes (a) and electrons (b) in 2T-BT, calculated from a DAD (ADA) oligomer triad at the B3LYP/6-31G(d) level, respectively.

Since the HOMO orbital of the acceptor moiety is antisymmetric while LUMO and LUMO+1 orbitals are symmetric, the sign of the denominator is the same as that of the numerator in eqn (11), constructive interference to the SE coupling. However, in the case of electron transport where the LUMO of acceptors is concerned, the LUMO and HOMO−3 orbitals of the bridge moiety (donor) are symmetric, while HOMO and LUMO+1 are antisymmetric. Thus, LUMO+1 and HOMO−3 of the bridge are destructive interference to the SE coupling. Thus, the SE of holes (382 meV) is much larger than that of electrons (173 meV) for 2T-BT. Electron transport would be further suppressed due to the injection barrier for these D–A copolymers, except for NDI and IID based copolymers. Thereafter, we focus on hole transport in these D–A copolymers.

It is clear from Fig. 4(b) that hole SE couplings increase linearly with the charge density of the HOMO at the linkage site, as expected from eqn (11). The CDT moiety reveals the largest charge density at the linking atom, and the CDT based copolymers display the largest SE coupling. For the Py moiety, however, there is no p_z atomic orbital coefficient in the linear combination of atomic orbitals (LCAO) expansion and little charge density distribution on linking carbon atoms due to the symmetry of the HOMO orbital (linkage atom at the node of the orbital), as shown in Table S4 and Fig. S3 (ESI†); therefore, when the Py moiety is coupled with acceptors, small SE coupling and a large effective mass are revealed, as can be seen in Fig. 2.

The ability of the bridge part to mediate the super-exchange interaction correlates with multi-orbital contribution. For hole transport, the HOMO level of the donor lies within the HOMO–LUMO gap of the bridge part. Both the HOMO and LUMO of the

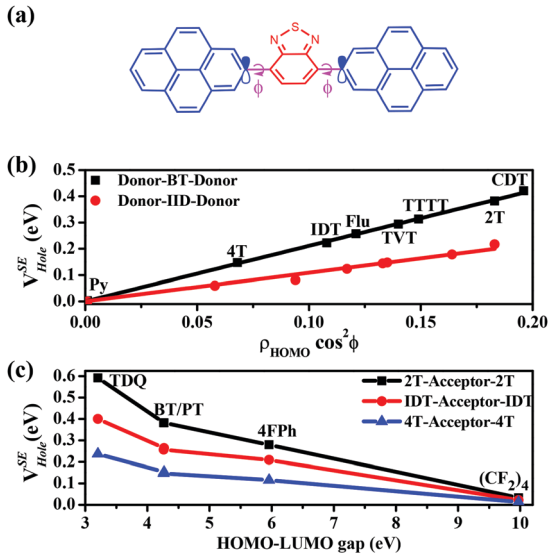

Fig. 4 (a) Oligomer triad model for hole SE coupling calculations. (b) The hole SE coupling as a function of charge density of the linkage atom. (c) The hole SE coupling dependence on the HOMO–LUMO gap of the bridge.

bridge play an important role in SE coupling. The bridge moiety having high frontier orbital charge density on linking atoms is a good building block for high performance D–A copolymers, as shown in Table S4 (ESI†).

The HOMO–LUMO gap of the bridge moiety has a great influence on SE coupling. The SE couplings monotonically decrease with the increase in the HOMO–LUMO gap, as can be seen from Fig. 4(c). Due to the nearly equal bandgap between BT and PT, similar SE coupling and effective masses can be obtained for BT and PT based copolymers, which is consistent with the experimentally reported charge mobility for BT and PT based copolymers.[6] Compared with the IID, BT and PT moiety, TDQ based copolymers with the smallest HOMO–LUMO gap display the largest SE coupling and the smallest effective mass.

Conclusions

Based on extensive first-principles computations on the effective mass, we propose here a super-exchange (SE) model to describe carrier transport in donor–acceptor copolymers. It has been successfully established that intrinsically D–A copolymers can possess small effective mass due to long-range super-exchange interactions, which rationalizes the recent experimental demonstration of ultra-high charge mobility in IDT-BT and CDT-PT (BT). The Py- and Flu-based copolymers demonstrate relatively small SE coupling strengths and large effective masses, which is consistent with the relatively low charge mobility in FET measurements. Moreover, it is also noted that the intra-chain effective mass is closely related to the measured charge transport properties and can be fully revealed from a SE perspective. The SE coupling strength is found to be determined by the dihedral angle between the donor (acceptor) moieties, frontier orbital charge densities at the donor and acceptor linkage sites, and the energy gap of the bridge part. The phases of the molecular orbital wavefunction also contribute to the SE coupling, as demonstrated by a tight-binding model.

We propose the following design strategy for high performance charge transport polymers: firstly, a coplanar backbone conformation with minimum backbone torsion and steric hindrance between the donor and acceptor moiety; secondly, for hole transport, a delocalized HOMO molecular orbital with high charge density at the linkage site adjacent to the acceptor (donor) moiety; and finally, the bridge fragments should possess a HOMO–LUMO gap as small as possible.

By combining a variety of donor and acceptor groups, a series of D–A copolymers which potentially possess ultra-low effective masses can be designed, such as TDQ based copolymers, which surpass CDT-PT with the smallest effective mass reported so far. This study provides molecular insights into the origin of electronic couplings in alternating D–A copolymers, paving the way toward rational design of high-performance charge transport polymers.

Acknowledgements

This work is supported by the National Natural Science Foundation of China (Grant Numbers: 21673247, 21290190, and 91333202), the Ministry of Science and Technology of China through 973 program (Grant No. 2013CB834703) and the Strategic Priority Research Program of the Chinese Academy of Sciences (Grant No. XDB12020200). The computational work was carried out in the CNIC supercomputer centre of the Chinese Academy of Sciences and the Tsinghua University High Performance Computing Centre.

Notes and references

1 R. C. Huber, A. S. Ferreira, R. Thompson, D. Kilbride, N. S. Knutson, L. S. Devi, D. B. Toso, J. R. Challa, Z. H. Zhou, Y. Rubin, B. J. Schwartz and S. H. Tolbert, *Science*, 2015, **348**, 1340.
2 D. Venkateshvaran, M. Nikolka, A. Sadhanala, V. Lemaur, M. Zelazny, M. Kepa, M. Hurhangee, A. J. Kronemeijer, V. Pecunia, I. Nasrallah, I. Romanov, K. Broch, I. McCulloch, D. Emin, Y. Olivier, J. Cornil, D. Beljonne and H. Sirringhaus, *Nature*, 2014, **515**, 384.
3 G. Kim, S. J. Kang, G. K. Dutta, Y. K. Han, T. J. Shin, Y. Y. Noh and C. Yang, *J. Am. Chem. Soc.*, 2014, **136**, 9477.
4 J. Yao, C. Yu, Z. Liu, H. Luo, Y. Yang, G. Zhang and D. Zhang, *J. Am. Chem. Soc.*, 2016, **138**, 173.
5 X. Zhang, H. Bronstein, A. J. Kronemeijer, J. Smith, Y. Kim, R. J. Kline, L. J. Richter, T. D. Anthopoulos, H. Sirringhaus, K. Song, M. Heeney, W. Zhang, I. McCulloch and D. M. DeLongchamp, *Nat. Commun.*, 2013, **4**, 2238.
6 C. Luo, A. K. Kyaw, L. A. Perez, S. Patel, M. Wang, B. Grimm, G. C. Bazan, E. J. Kramer and A. J. Heeger, *Nano Lett.*, 2014, **14**, 2764.
7 R. A. Street, *Science*, 2013, **341**, 1072.

8 J. D. Yuen, J. Fan, J. Seifter, B. Lim, R. Hufschmid, A. J. Heeger and F. Wudl, *J. Am. Chem. Soc.*, 2011, **133**, 20799.
9 J. Lee, J. W. Chung, H. Kim do, B. L. Lee, J. I. Park, S. Lee, R. Hausermann, B. Batlogg, S. S. Lee, I. Choi, I. W. Kim and M. S. Kang, *J. Am. Chem. Soc.*, 2015, **137**, 7990.
10 H. J. Yun, S. J. Kang, Y. Xu, S. O. Kim, Y. H. Kim, Y. Y. Noh and S. K. Kwon, *Adv. Mater.*, 2014, **26**, 7300.
11 B. Sun, W. Hong, Z. Yan, H. Aziz and Y. Li, *Adv. Mater.*, 2014, **26**, 2636.
12 C. Xiao, G. Zhao, A. Zhang, W. Jiang, R. A. Janssen, W. Li, W. Hu and Z. Wang, *Adv. Mater.*, 2015, **27**, 4963.
13 A. Luzio, D. Fazzi, D. Natali, E. Giussani, K.-J. Baeg, Z. Chen, Y.-Y. Noh, A. Facchetti and M. Caironi, *Adv. Funct. Mater.*, 2014, **24**, 1151.
14 I. McCulloch, M. Heeney, M. L. Chabinyc, D. DeLongchamp, R. J. Kline, M. Cölle, W. Duffy, D. Fischer, D. Gundlach, B. Hamadani, R. Hamilton, L. Richter, A. Salleo, M. Shkunov, D. Sparrowe, S. Tierney and W. Zhang, *Adv. Mater.*, 2009, **21**, 1091.
15 R. P. Fornari and A. Troisi, *Adv. Mater.*, 2014, **26**, 7627.
16 B. B. Hsu, C. M. Cheng, C. Luo, S. N. Patel, C. Zhong, H. Sun, J. Sherman, B. H. Lee, L. Ying, M. Wang, G. Bazan, M. Chabinyc, J. L. Bredas and A. Heeger, *Adv. Mater.*, 2015, **27**, 7759.
17 S. P. Senanayak, A. Z. Ashar, C. Kanimozhi, S. Patil and K. S. Narayan, *Phys. Rev. B: Condens. Matter Mater. Phys.*, 2015, **91**, 115302.
18 S. Schott, E. Gann, L. Thomsen, S. H. Jung, J. K. Lee, C. R. McNeill and H. Sirringhaus, *Adv. Mater.*, 2015, **27**, 7356.
19 Y. Yamashita, J. Tsurumi, F. Hinkel, Y. Okada, J. Soeda, W. Zajaczkowski, M. Baumgarten, W. Pisula, H. Matsui, K. Mullen and J. Takeya, *Adv. Mater.*, 2014, **26**, 8169.
20 M. Mladenović and N. Vukmirović, *Adv. Funct. Mater.*, 2015, **25**, 1915.
21 H. Sirringhaus, *Adv. Mater.*, 2014, **26**, 1319.
22 H. A. Um, D. H. Lee, D. U. Heo, D. S. Yang, J. Shin, H. Baik, M. Cho and D. H. Choi, *ACS Nano*, 2015, **9**, 5264.
23 N. E. Jackson, K. L. Kohlstedt, B. M. Savoie, M. O. de la Cruz, G. C. Schatz, L. X. Chen and M. A. Ratner, *J. Am. Chem. Soc.*, 2015, **137**, 6254.
24 R. Dovesi, R. Orlando, A. Erba, C. M. Zicovich-Wilson, B. Civalleri, S. Casassa, L. Maschio, M. Ferrabone, M. De La Pierre, P. D'Arco, Y. Noël, M. Causà, M. Rérat and B. Kirtman, *Int. J. Quantum Chem.*, 2014, **114**, 1287.
25 L. Zhu, Y. Yi, Y. Li, E. G. Kim, V. Coropceanu and J. L. Bredas, *J. Am. Chem. Soc.*, 2012, **134**, 2340.
26 H. Geng, X. Zheng, Z. Shuai, L. Zhu and Y. Yi, *Adv. Mater.*, 2015, **27**, 1443.
27 G. W. T. M. J. Frisch, H. B. Schlegel, G. E. Scuseria, M. A. Robb, J. R. Cheeseman, G. Scalmani, V. Barone, B. Mennucci, G. A. Petersson, H. Nakatsuji, M. Caricato, X. Li, H. P. Hratchian, A. F. Izmaylov, J. Bloino, G. Zheng, J. L. Sonnenberg, M. Hada, M. Ehara, K. Toyota, R. Fukuda, J. Hasegawa, M. Ishida, T. Nakajima, Y. Honda, O. Kitao, H. Nakai, T. Vreven, J. A. Montgomery, Jr., J. E. Peralta, F. Ogliaro, M. Bearpark, J. J. Heyd, E. Brothers, K. N. Kudin, V. N. Staroverov, R. Kobayashi, J. Normand, K. Raghavachari, A. Rendell, J. C. Burant, S. S. Iyengar, J. Tomasi, M. Cossi, N. Rega, J. M. Millam, M. Klene, J. E. Knox, J. B. Cross, V. Bakken, C. Adamo, J. Jaramillo, R. Gomperts, R. E. Stratmann, O. Yazyev, A. J. Austin, R. Cammi, C. Pomelli, J. W. Ochterski, R. L. Martin, K. Morokuma, V. G. Zakrzewski, G. A. Voth, P. Salvador, J. J. Dannenberg, S. Dapprich, A. D. Daniels, Ö. Farkas, J. B. Foresman, J. V. Ortiz, J. Cioslowski and D. J. Fox, Gaussian Inc., Wallingford, CT, 2009.
28 T. Lei, J. Y. Wang and J. Pei, *Acc. Chem. Res.*, 2014, **47**, 1117.
29 X. Liu, Y. Guo, Y. Ma, H. Chen, Z. Mao, H. Wang, G. Yu and Y. Liu, *Adv. Mater.*, 2014, **26**, 3631.
30 D. Niedzialek, V. Lemaur, D. Dudenko, J. Shu, M. R. Hansen, J. W. Andreasen, W. Pisula, K. Muellen, J. Cornil and D. Beljonne, *Adv. Mater.*, 2013, **25**, 1939.
31 G.-J. A. Wetzelaer, M. Kuik, Y. Olivier, V. Lemaur, J. Cornil, S. Fabiano, M. A. Loi and P. W. Blom, *Phys. Rev. B: Condens. Matter Mater. Phys.*, 2012, **86**, 165203.
32 W. Zhong, J. Liang, S. Hu, X.-F. Jiang, L. Ying, F. Huang, W. Yang and Y. Cao, *Macromolecules*, 2016, **49**, 5806.
33 G. E. Park, J. Shin, D. H. Lee, T. W. Lee, H. Shim, M. J. Cho, S. Pyo and D. H. Choi, *Macromolecules*, 2014, **47**, 3747.
34 D. Wang, W. Shi, J. Chen, J. Xi and Z. Shuai, *Phys. Chem. Chem. Phys.*, 2012, **14**, 16505.
35 J. E. Northrup, *Phys. Rev. B: Condens. Matter Mater. Phys.*, 2007, **76**, 245202.
36 M. M. Szumilo, E. H. Gann, C. R. McNeill, V. Lemaur, Y. Oliver, L. Thomsen, Y. Vaynzof, M. Sommer and H. Sirringhaus, *Chem. Mater.*, 2014, **26**, 6796.
37 M. C. Gwinner, F. Jakubka, F. Gannott, H. Sirringhaus and J. Zaumseil, *ACS Nano*, 2012, **6**, 539.
38 Y. Kim, J. Hong, J. H. Oh and C. Yang, *Chem. Mater.*, 2013, **25**, 3251.